
Predictive Modeling of Coronal Hole Areas Using Long Short-Term Memory Networks

Juyoung Yun

Department of Computer Science
Stony Brook University
juyoung.yun@stonybrook.edu

Abstract

In the era of space exploration, the implications of space weather have become increasingly evident. Central to this is the phenomenon of coronal holes, which can significantly influence the functioning of satellites and aircraft. These coronal holes, present on the sun, are distinguished by their open magnetic field lines and comparatively cooler temperatures, leading to the emission of solar winds at heightened rates. To anticipate the effects of these coronal holes on Earth, our study harnesses computer vision to pinpoint the coronal hole regions and estimate their dimensions using imagery from the Solar Dynamics Observatory (SDO). Further, we deploy deep learning methodologies, specifically the Long Short-Term Memory (LSTM) approach, to analyze the trends in the data related to the area of the coronal holes and predict their dimensions across various solar regions over a span of seven days. By evaluating the time series data concerning the area of the coronal holes, our research seeks to uncover patterns in the behavior of coronal holes and comprehend their potential influence on space weather occurrences. This investigation marks a pivotal stride towards bolstering our capacity to anticipate and brace for space weather events that could have ramifications for Earth and its technological apparatuses.

Keywords: Space Weather, Coronal Hole, Deep Learning, Time Series Prediction

1 Introduction

The exploration of space has underscored the importance of understanding space weather phenomena, especially those related to coronal holes [12, 47]. These regions on the sun, characterized by open magnetic field lines and cooler temperatures, emit solar winds at higher rates than their surroundings. Such emissions have profound implications for Earth, influencing operations of aircraft, satellites, and even terrestrial technologies [15, 44].

Space weather, driven by solar activities, affects the vast expanse between the Sun and Earth, encompassing the solar wind, Earth's magnetosphere, ionosphere, and thermosphere [39]. Phenomena like solar flares and coronal mass ejections are pivotal in shaping space weather, with consequences ranging from satellite communication disruptions to compromised GPS signal accuracy [44, 48].

While the significance of coronal holes in influencing space weather is well-established, there exists a gap in the literature concerning the prediction of their size and evolution. Accurate prediction of coronal hole dimensions is pivotal, as their size and position can directly influence the intensity and impact of solar wind streams on Earth [9, 29].

Addressing this research gap, our study introduces a novel approach that combines computer vision techniques with deep learning methodologies to predict the size of coronal holes. Our methodology offers:

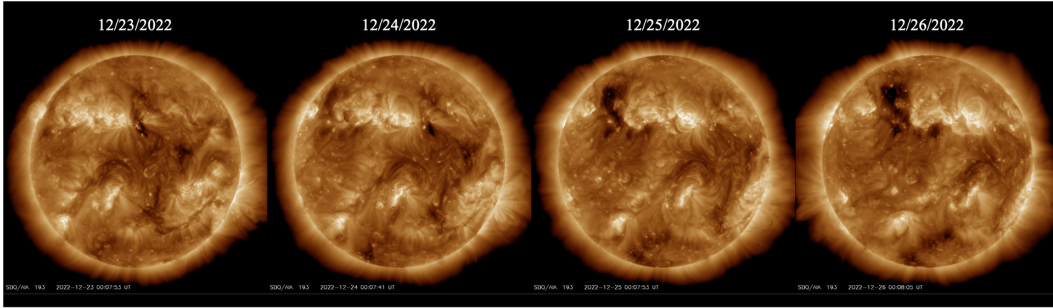


Figure 1: A visual representation of the changes in coronal hole size and position over a 4-day period from December 23, 2022 to December 26, 2022, as captured by the NASA Heliophysics Integrated Observatory Network. The image illustrates the dynamic nature of coronal holes and their potential impact on space weather events.

- **Accuracy and Consistency:** Through computer vision, we ensure objective and consistent detection, eliminating the inconsistencies of manual inspection.
- **Efficiency:** Our automated approach drastically reduces the time and effort required for detection compared to traditional methods.
- **Predictive Power:** By harnessing the capabilities of the Long Short-Term Memory (LSTM) model, we can forecast the size of coronal holes over a week, providing invaluable insights into impending space weather events.
- **Scalability:** Our approach is versatile, allowing for analysis across extensive datasets and offering insights into long-term patterns of coronal hole evolution.

In essence, our research endeavors to provide a comprehensive understanding of coronal hole behavior, aiming to bolster our predictive capabilities for space weather events that have far-reaching implications for Earth's technological infrastructure [39].

2 Background

2.1 Coronal Hole Examination

Utilizing extreme ultraviolet (EUV) wavelengths, we can observe coronal holes, which are emitted by the sun's hot, low-density plasma in the corona [30]. Instruments like the Atmospheric Imaging Assembly (AIA) on the Solar Dynamics Observatory (SDO) spacecraft, launched by NASA in 2010, facilitate these observations [30, 38]. The AIA 193 channel, specifically designed for EUV wavelength observations, aids in studying the sun's atmosphere and solar eruptions dynamics [38]. Fig 1 showcases the sun's atmosphere observed at a wavelength of 193 angstroms. Computational models, such as magnetohydrodynamic (MHD) or potential field source surface (PFSS) models, also aid in detecting coronal holes by simulating the sun's magnetic field and plasma behavior [26].

2.2 Solar Plasma Eruptions

Coronal mass ejections (CMEs) are significant solar plasma and magnetic field discharges from the Sun's corona into space [52]. These eruptions, often linked with solar flares, are believed to be the result of energy release from the Sun's magnetic field [52]. CMEs can influence Earth's space environment, leading to geomagnetic storms that alter the Earth's ionosphere, magnetosphere, and geomagnetic field [48].

2.3 Solar Wind Interactions

Corotating interaction regions (CIRs) are characterized by swift alterations in solar wind's plasma and magnetic field [23]. Originating from the interaction between varying speed solar wind streams, CIRs, when reaching Earth, can induce geomagnetic storms, affecting Earth's space environment and

technological systems [48]. Recognizing CIRs' formation and progression is pivotal for forecasting their Earthly impacts.

CME frequency peaks during solar maximum periods [52], leading to CME-caused storms [46]. Well-formed Corotating Interaction Regions (CIRs) with 27-day recurrences are more frequent during the solar cycle's later stages [36]. Interaction Regions (IRs) can cause non-recurring geomagnetic activity throughout the solar cycle [7, 45].

2.4 Magnetospheric Disturbances

Geomagnetic storms, disturbances in Earth's magnetosphere, arise from high-speed solar wind streams from the sun's coronal holes [13]. These storms can influence navigation systems, satellite communications, and GPS signal accuracy [15, 44]. The Kp index measures geomagnetic storm intensity, with storms having a Kp index of 5 or above considered significant [38]. These storms can also generate auroras, visible at high latitudes [44]. Various geomagnetic indices, like the auroral electrojet (AE) index and disturbance storm time (Dst) index, gauge the impact of solar events on Earth [2].

2.5 Coronal Hole Influence and AP Index

Introduced by Bartels [5], the standardized Ks and planetary Kp indices measure geomagnetic activity, recorded every three hours [4]. The AP index, derived from KP, gauges geomagnetic activity intensity on Earth, resulting from the interaction between Earth's magnetosphere and the solar wind [13, 44]. Strong CIRs and faster CH HSS can induce geomagnetic storms, classified using the NOAA Space Weather Scale [11]. The AP index quantifies geomagnetic activity, helping assess space weather events' potential impacts on Earth, based on auroral oval boundary crossings observed globally [40].

2.6 Related Works

Coronal Hole Detection: Historically, the primary focus in the domain of coronal hole research has been on detection. Various methodologies, ranging from manual inspection to automated computer vision techniques, have been employed to identify these regions on the sun. For instance, several studies have utilized image processing techniques on data from observatories to detect the cooler and less dense regions that characterize coronal holes. While these methods have been successful in identifying the presence of coronal holes, they often do not provide insights into the future behavior or evolution of these regions.

In recent advancements, Linker et al. [32] presented a deep learning approach using a U-Net architecture to detect coronal holes in solar images. Their method emphasizes the potential of deep learning in improving space weather forecasting. Similarly, Jarolim et al. [27] introduced a convolutional neural network model named CHRONNOS, which utilizes multi-channel data for precise coronal hole boundary detection. Their approach showcases the potential of CNNs in providing reliable coronal hole detections suitable for real-time applications. While these methods significantly improved the detection accuracy, the focus remained primarily on identification rather than prediction.

Lack of Predictive Models: One of the significant gaps in the existing literature is the absence of robust predictive models for coronal holes. While detection models are abundant, very few, if any, studies have delved into predicting the future size, shape, or behavior of coronal holes. This is a crucial distinction as understanding the future behavior of these holes can provide insights into potential space weather events, which can have profound implications for Earth-based technologies.

Novelty of Our Approach: Our research introduces a pioneering approach to this domain by not only detecting but also predicting the dimensions of coronal holes. By employing the Long Short-Term Memory (LSTM) model, we harness the power of deep learning to forecast the area of the coronal hole in the Sun's middle region over a span of seven days. This predictive capability is a significant advancement in the field and addresses a critical gap in the existing literature. The ability to anticipate the behavior of coronal holes can provide valuable lead time for preparations against potential space weather events.

In conclusion, while there have been substantial efforts in the detection of coronal holes, the predictive aspect remains largely unexplored. Our research fills this void by introducing a novel methodology

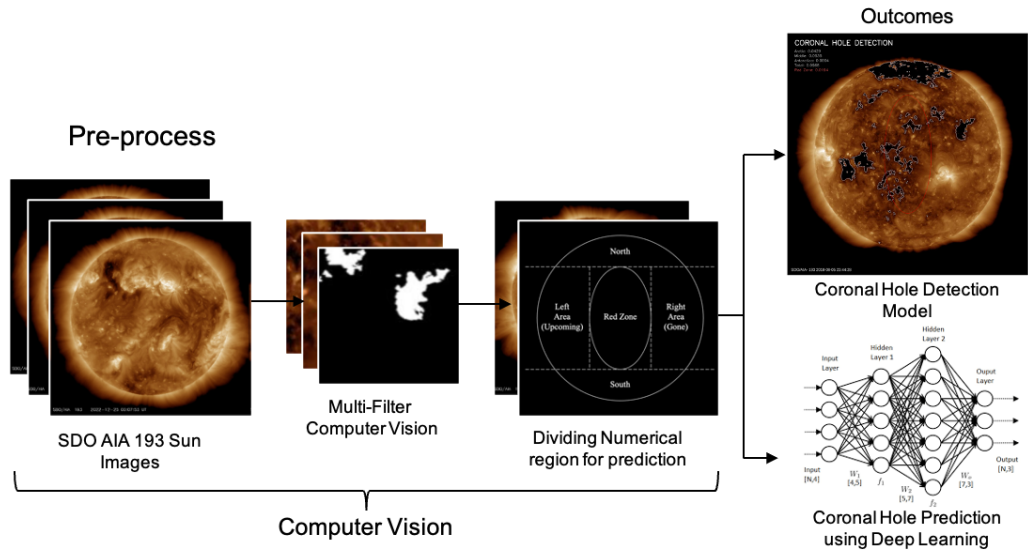


Figure 2: The regions used to determine the coronal hole area in the sun, as defined by the binary-based Coronal Hole Detection model (BCH). The original AIA image, sourced from the NASA Heliophysics Integrated Observatory Network, highlights various regions for coronal hole area calculation.

that promises enhanced predictive accuracy, positioning our work as a groundbreaking contribution to the field.

3 Method

In this study, we introduce a novel approach to predict the area of the coronal hole by leveraging computer vision techniques and deep learning models. Our methodology can be broadly divided into two main phases: Coronal Hole Detection using computer vision and Time Series Prediction using deep learning.

As depicted in Figure 2, the first phase focuses on the detection of coronal holes. This is achieved through a series of computer vision techniques that process solar images, enhancing their features and converting them into a format suitable for analysis. The primary objective of this phase is to accurately identify and delineate the coronal hole regions in the images, ensuring that the data fed into the subsequent phase is precise.

The second phase, as shown on the right side of Figure 2, involves the application of a deep learning model to the data obtained from the first phase. This model is trained on time series data of the detected coronal hole areas, enabling it to predict future trends and variations in the size and position of the coronal holes. The combination of computer vision for detection and deep learning for prediction ensures a comprehensive and robust approach to understanding and forecasting the behavior of coronal holes.

3.1 Coronal Hole Detection using Computer Vision

Traditional identification of the coronal hole region relies on manual inspection, which can yield inconsistent results due to human subjectivity. To address this, we developed a computer vision model that automates the detection process, ensuring objective and consistent results. Fig 3 shows the coronal hole detection processes based on the computer vision technique.

3.1.1 Anti-Noising Techniques

To enhance the visibility of coronal holes in AIA 193 images, we employed anti-noising techniques, specifically the non-local means anti-noising (NLmeans) method. This method reduces ambiguous

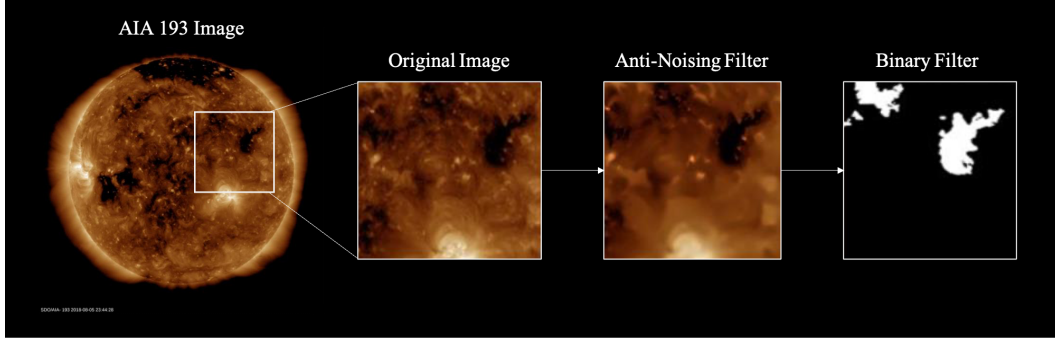


Figure 3: A depiction of the multi-filters computer vision based coronal hole detection techniques applied to an original AIA 193 image captured by the NASA Heliophysics Integrated Observatory Network. The image illustrates the use of various filters such as anti-noising and binary filters to accurately identify and measure the area of coronal holes in the sun.

and noisy areas in the images, making the black regions, which represent the coronal holes, more prominent. Fig 4 shows the original image and anti-noised image.

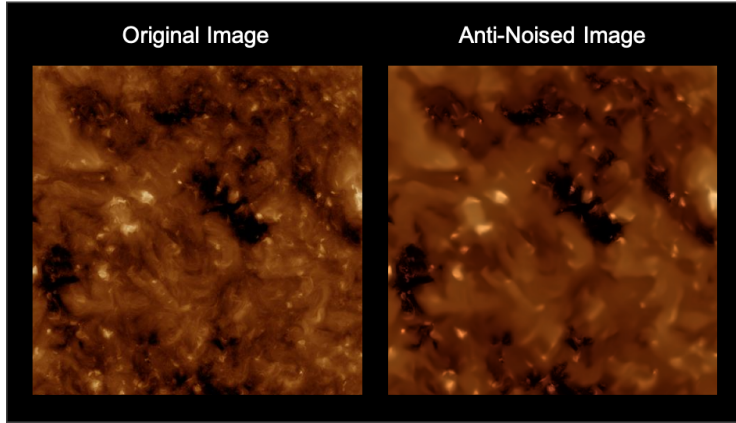


Figure 4: Original Image and Anti-noised Image (Original AIA 193 image courtesy The NASA Heliophysics Integrated Observatory Network)

The non-local means (NLmeans) anti-noising method is a sophisticated technique that leverages the redundancy of information in an image [10]. Unlike local methods, which only consider nearby pixels, NLmeans considers the entire image to determine the best way to denoise each pixel.

The NLmeans algorithm operates under the assumption that if two small patches in an image look similar, they should have similar denoised outputs. The mathematical representation of the NLmeans process is[10]:

$$J(x) = \frac{1}{W(x)} \sum_{y \in \Omega} I(y) \cdot K(x, y) \quad (1)$$

Where $K(x, y)$ is a weighting function that measures the similarity between patches centered at pixels x and y . The function is defined as:

$$K(x, y) = \exp \left(\frac{-\|I(x) - I(y)\|^2}{h^2} \right) \quad (2)$$

The parameter h controls the decay of the weights and effectively determines the degree of smoothing.

3.1.2 Image Binarization

Post noise-reduction, we applied image binarization to convert the AIA 193 images into binary form. This process transforms the coronal hole region to white, making it distinct from the rest of the solar

image. The threshold method was used for binarization, where pixels with values above a certain threshold are turned white, and those below are turned black. Fig 4 shows the original image and the binarized image.

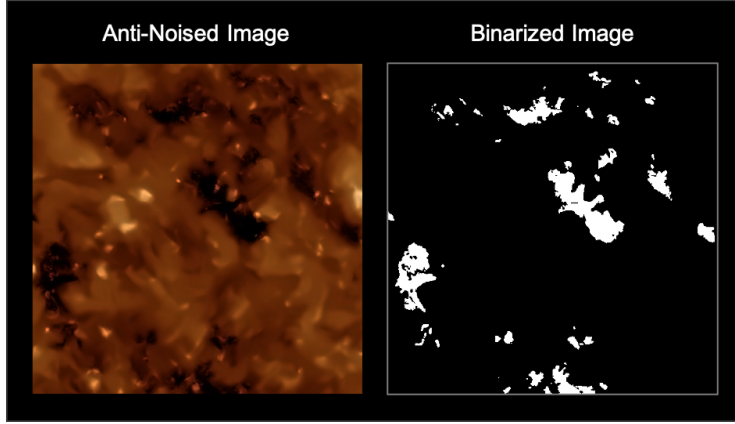


Figure 5: Anti-noised Image and Binarized Image (Original AIA 193 image courtesy The NASA Heliophysics Integrated Observatory Network)

Image binarization is a fundamental step in image processing, especially when the goal is to highlight specific features of an image. By converting an image into a binary format, we can easily differentiate between the regions of interest and the background.

The mathematical representation of the binarization process is [17]:

$$B(x, y) = \begin{cases} 1 & \text{if } I(x, y) > T \\ 0 & \text{otherwise} \end{cases} \quad (3)$$

Where T is a threshold value that determines the boundary between the two binary values.

3.1.3 Contour Detection

To further refine the detection, we employed the Laplacian of Gaussian (LoG) operator for edge detection[33]. This operator is sensitive to abrupt changes in image intensity, which often correspond to object boundaries in images. By contouring the coronal hole, we can easily delineate its area.

Contours are continuous curves that follow a boundary. Detecting these contours, especially in images with noise, requires sophisticated techniques. The Laplacian of Gaussian (LoG) is one such technique that first smoothens the image using a Gaussian filter and then finds the second derivative to detect the edges.

The LoG operator is mathematically represented as[33]:

$$L(x, y) = (x^2 + y^2 - \sigma^2) \cdot \frac{G(x, y)}{2\pi\sigma^4} \quad (4)$$

Where $G(x, y)$ is the Gaussian function:

$$G(x, y) = \frac{1}{2\pi\sigma^2} \exp\left(\frac{-(x^2 + y^2)}{2\sigma^2}\right) \quad (5)$$

The LoG operator is particularly effective because it is sensitive to rapid changes in intensity, which often correspond to the boundaries of objects in images.

3.2 Time Series Prediction using Deep Learning

While computer vision techniques allow for accurate detection of coronal holes, predicting their future behavior requires a different approach. Given the time-series nature of our data, we adopted deep learning techniques for this purpose.

3.2.1 Data Collection

We extracted daily coronal hole area data from AIA 193 images captured by NASA’s Solar Dynamics Observatory (SDO) over a span of 3857 days, from January 6, 2011, to August 10, 2021. The coronal hole area data for each day was obtained using our Binary-based Coronal Hole Detection model (BCH), which calculates the ratio of white areas (coronal holes) to the total area of the solar disk.

3.2.2 LSTM Model

Long Short-Term Memory (LSTM) networks[51], a subclass of Recurrent Neural Networks (RNNs), have been specifically engineered to address the challenges of long-term dependencies in sequential data. Given the time series nature of our dataset, which chronicles the areas of coronal holes, the LSTM model emerges as a fitting choice for predictive analysis.

The LSTM architecture is built around memory cells, which are adept at retaining or forgetting information based on the context. Each memory cell is regulated by three gates: the input gate, the forget gate, and the output gate. These gates determine how information flows into, within, and out of the memory cell. Detailed Mathematical Formulation[51]:

Input Gate (i_t): Determines the extent of new information to be stored in the cell state. It’s calculated as:

$$i_t = \sigma(W_{ii}x_t + b_{ii} + W_{hi}h_{t-1} + b_{hi})$$

Here, σ is the sigmoid activation function, which squashes values between 0 and 1, ensuring a gate value in this range.

Forget Gate (f_t): Decides the amount of past information (from the previous cell state) to be retained or discarded.

$$f_t = \sigma(W_{if}x_t + b_{if} + W_{hf}h_{t-1} + b_{hf})$$

Output Gate (o_t): Controls the amount of information from the current cell state to be outputted to the hidden state.

$$o_t = \sigma(W_{io}x_t + b_{io} + W_{ho}h_{t-1} + b_{ho})$$

New Cell Information (\tilde{c}_t): Represents the new information to be potentially added to the cell state.

$$\tilde{c}_t = \tanh(W_{ic}x_t + b_{ic} + W_{hc}h_{t-1} + b_{hc})$$

The tanh function outputs values between -1 and 1, providing a normalized weight to the new information.

Cell State Update (c_t): Combines the past cell state with the new cell information, modulated by the input and forget gates.

$$c_t = f_t \odot c_{t-1} + i_t \odot \tilde{c}_t$$

Here, \odot denotes element-wise multiplication.

Hidden State Update (h_t): Determines the output hidden state based on the current cell state and the output gate.

$$h_t = o_t \odot \tanh(c_t)$$

Notations:

- x_t : Represents the input vector at the current time step t .
- W and b : Denote the weight matrices and bias vectors associated with each gate.
- σ : The sigmoid activation function, which outputs values between 0 and 1.
- \odot : Symbolizes element-wise multiplication.
- \tanh : The hyperbolic tangent activation function, producing values between -1 and 1.

In essence, the LSTM’s intricate design, characterized by its gates and memory cells, equips it with the capability to judiciously manage information flow. This ensures that it can effectively handle sequences with long-term dependencies, making informed decisions on what information to retain, update, or discard based on the prevailing context.

3.2.3 Advantages and Suitability of LSTM for Our Research

Long Short-Term Memory (LSTM) networks, being a specialized form of Recurrent Neural Networks (RNNs), offer several advantages that make them particularly suited for our research on predicting the area of coronal holes based on time series data:

- **Handling Sequential Data:** LSTMs are inherently designed to process sequential data. Given that our dataset chronicles the areas of coronal holes over time, the sequential nature of LSTMs makes them a natural fit. In contrast, Convolutional Neural Networks (CNNs) are primarily designed for spatial hierarchies, making them ideal for image data but less so for time series data.
- **Long-term Dependencies:** One of the primary strengths of LSTMs is their ability to remember and leverage long-term dependencies in data. This is crucial for our research, as past observations of coronal holes can significantly influence future predictions. Traditional RNNs struggle with this aspect due to the vanishing gradient problem, but LSTMs effectively address this issue with their gating mechanisms.
- **Avoiding the Vanishing Gradient Problem:** LSTMs, with their unique architecture, can mitigate the vanishing gradient problem that plagues traditional RNNs. This ensures that they can effectively learn from earlier time steps, even in long sequences.
- **Flexibility:** LSTMs can be easily retrained with new data, allowing them to adapt to evolving patterns in the coronal hole areas over time. This adaptability ensures that the model remains relevant and accurate as more data becomes available.
- **Interpretability:** The sequential nature of LSTMs, combined with their ability to weigh the importance of different inputs at different time steps, offers a clearer understanding of how past data points influence future predictions. This level of transparency can be more challenging to achieve with some deep learning models, especially deep CNNs.
- **Efficiency:** While deep CNNs might require more layers and, consequently, more computational resources, especially when dealing with large images, LSTMs can efficiently process long sequences without necessitating extensive computational power.

Why LSTM over CNN or Other Deep Learning Models? While CNNs have proven effective in many applications, especially those involving image data, their primary strength lies in recognizing spatial patterns. Our research, however, is centered around recognizing temporal patterns in time series data, a domain where LSTMs excel. Additionally, other deep learning models might not offer the same level of efficiency, flexibility, and interpretability as LSTMs, especially when dealing with long-term dependencies in sequential data.

In conclusion, the choice of LSTM for our research is not only driven by its inherent strengths but also by its clear advantages over other potential models for this specific application.

4 Data Analysis

5 Analysis

Before embarking on the intricate journey of deep learning predictions, it's imperative to underscore the significance of data extraction and analysis. The BCH model serves as our cornerstone in this endeavor, ensuring that the data we feed into our predictive algorithms is both accurate and meaningful. By meticulously analyzing the data through the BCH model, we lay a robust foundation for subsequent deep learning applications, ensuring that our predictions are grounded in reality and are of practical relevance.

Fig. 6 provides a comprehensive view of the coronal hole areas on the sun, specifically on August 10, 2021, juxtaposed with data spanning back to January 6, 2011. A discernible trend emerges from this analysis: the coronal hole area has been on a gradual incline over the past decade. The middle region, in particular, has witnessed a pronounced expansion, hinting at the possibility of the coronal hole widening its expanse. However, a caveat remains: a decade, in the grand scheme of solar dynamics, is a relatively short window. For a more holistic understanding of the coronal hole's behavior, a more extended dataset would be invaluable.

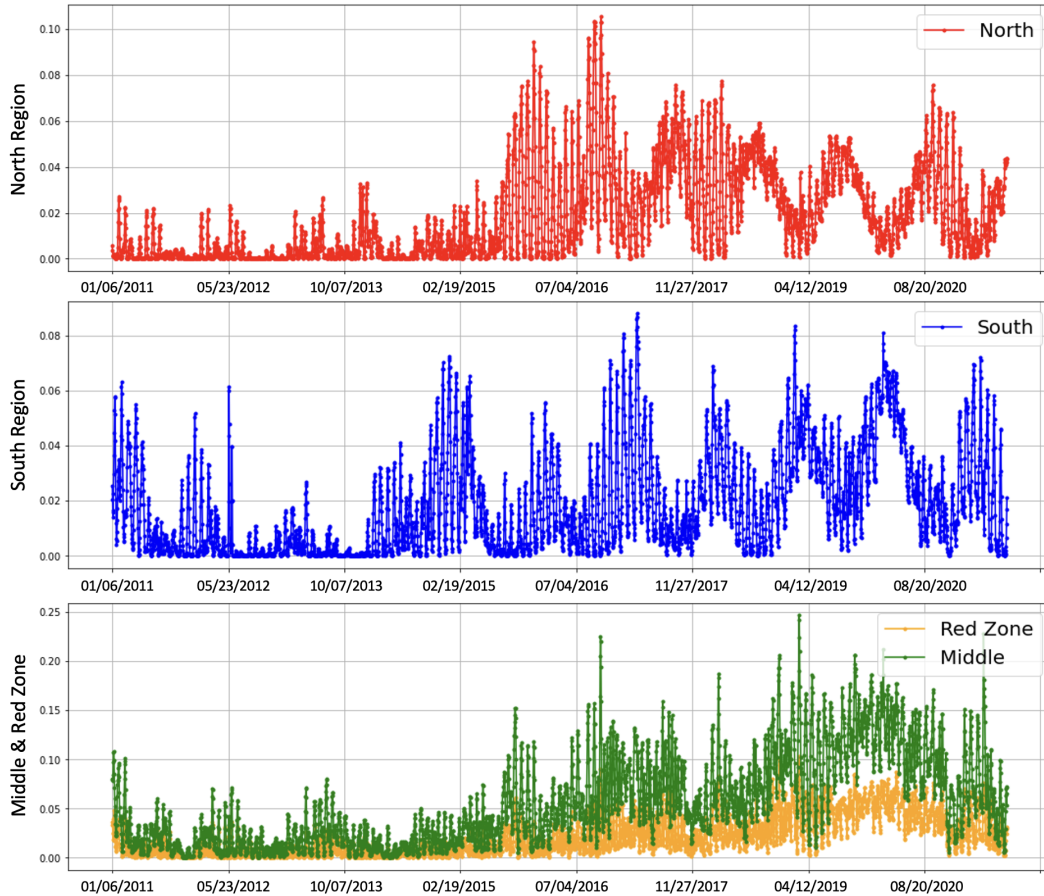


Figure 6: Daily Coronal Hole Data for each region of the sun, calculated over a period of 3857 days from January 6, 2011 to August 10, 2021, obtained by the binary-based Coronal Hole Detection model (BCH). The graph presents the variation of coronal hole area for each regions of the sun over time.

Solar scholars have long been intrigued by the sun’s corona, a region known for its dynamism and frequent flux. Coronal hole expansions have been observed to be in tandem with the solar cycle, an 11-year cycle punctuated by the ebb and flow of solar activities like sunspots, flares, and coronal mass ejections. The expansion observed in our study might be tethered to the current phase of this solar cycle. However, establishing this causal link necessitates further probing.

Fig. 8 delves into the relationship between the AP index and the coronal hole areas in the middle and red zone regions of the sun over a 50-day period. The graph underscores a correlation, suggesting that as the coronal hole area swells, the AP index follows suit after a short lag. This observation is pivotal as it hints at the potential of using coronal hole areas as a predictor for geomagnetic disturbances.

5.1 Pole Region Analysis

Fig. 7 offers a panoramic view of the coronal hole areas over a 1000-day trajectory. A striking observation emerges: the coronal hole areas in the sun’s north and south pole regions often exhibit opposing behaviors. This phenomenon, termed the "polarity rule," aligns with previous findings that coronal holes near the sun’s poles often have opposing magnetic field configurations and produce solar wind streams that move in opposite directions. The sun’s magnetic field orientation is responsible for this, deflecting solar wind particles in contrasting directions at the poles.

Our findings bolster the claims of prior research that delved into the polarities of coronal holes and their interplay with solar wind streams. By providing a comprehensive dataset spanning 1000 days and underscoring the consistency of the polarity rule, our study enriches the current understanding of

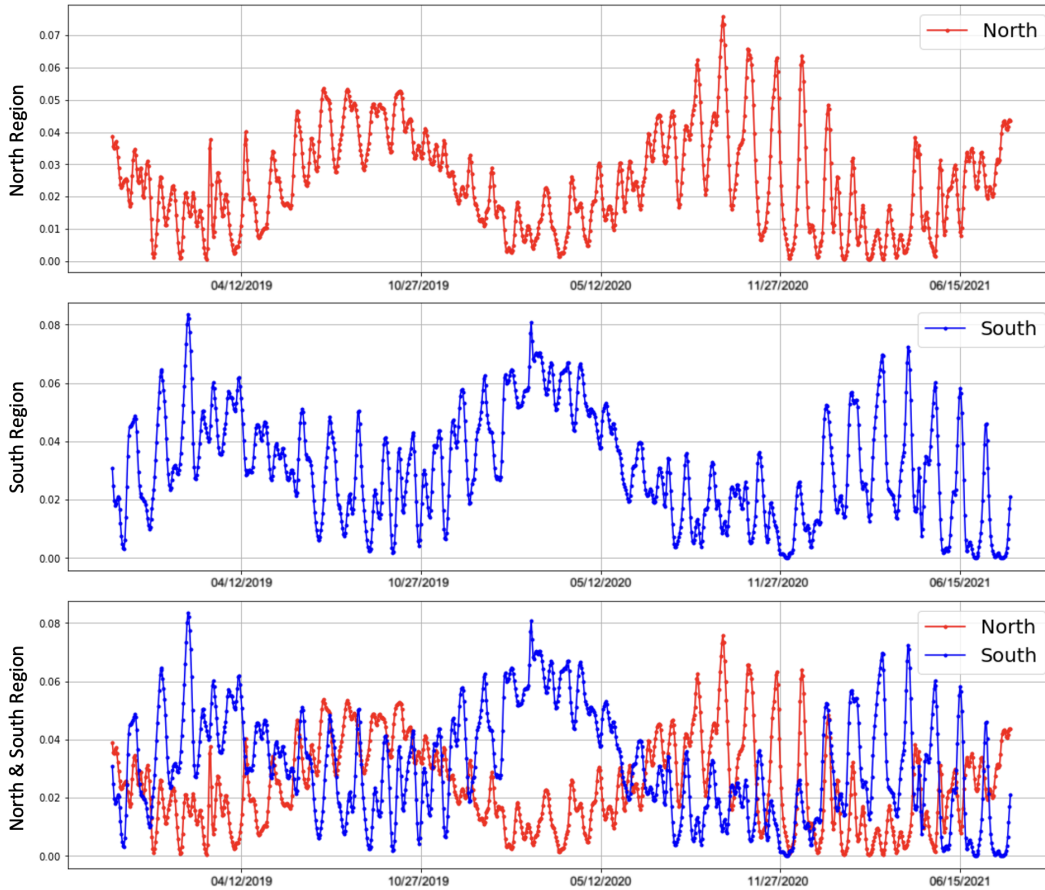


Figure 7: A comparison of daily coronal hole data for the south and north regions of the sun over a 1000-day period from November 13, 2018 to August 10, 2021 as obtained by the binary-based Coronal Hole Detection model (BCH). The graph illustrates the variation of coronal hole area in the south and north regions over time, and the consistency of the polarity rule.

coronal hole dynamics. However, the 1000-day window, while insightful, is relatively short. A more extended dataset would offer a more nuanced understanding of the coronal hole’s behavior and its interplay with the solar cycle.

5.2 Middle Region Analysis

The middle region of the sun holds significant importance when it comes to anticipating geomagnetic disturbances on Earth. These disturbances, gauged by the AP index, can be triggered by high-speed solar wind streams emanating from coronal holes [55]. Such disturbances can wreak havoc, causing power grid failures [8], communication disruptions, satellite damage [3], and more. Our research aimed to unearth the relationship between the coronal hole’s size in the middle region and Earth’s geomagnetic activity.

Our BCH model, built on AIA 193 images from NASA’s Solar Dynamics Observatory [43], has proven instrumental in this endeavor. The model’s accuracy in measuring coronal hole areas has enabled us to establish a robust correlation between the size of the coronal hole in the middle region and Earth’s geomagnetic activity. Specifically, a surge in the coronal hole size often precedes a spike in the AP index by 3-4 days.

Fig. 8 further elucidates this relationship. Rapid expansions in the red zone and middle area are often precursors to a subsequent rise in the AP index [21]. Such expansions are typically triggered by solar activities like solar flares [28] or coronal mass ejections [20], which can disrupt Earth’s

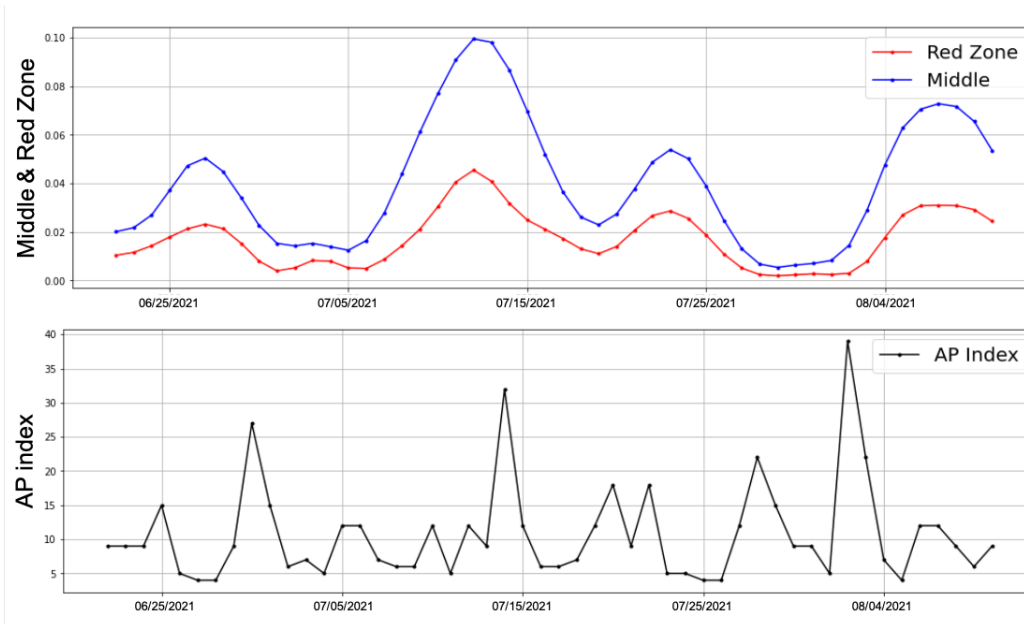


Figure 8: The AP index and the data calculated for the middle and redzone regions of coronal hole on the sun for a period of 50 days from June 22, 2021 to August 10, 2021, as obtained by the binary-based Coronal Hole Detection model (BCH). The graph illustrates the correlation between the AP index and the coronal hole area in the middle and redzone regions of the sun. (AP index data courtesy of World Data Center for Geomagnetism, Kyoto)

magnetosphere [18]. Monitoring these areas, coupled with other solar activity indicators, is paramount to anticipate and brace for potential AP index surges [41].

5.3 Summary of Insights

The comprehensive analysis, underpinned by the BCH model and spanning over a decade, has unveiled several pivotal insights into the behavior of coronal holes and their implications for Earth:

- **Temporal Expansion of Coronal Holes:** The data, as visualized in Fig. 6, underscores a gradual expansion of the coronal hole areas over the past decade. This trend, especially pronounced in the middle region, hints at the dynamic nature of the sun's corona and the potential widening of the coronal hole.
- **Correlation with Geomagnetic Disturbances:** The middle region of the sun, as depicted in Fig. 8, plays a crucial role in influencing geomagnetic disturbances on Earth. A surge in the coronal hole size in this region often heralds a spike in the AP index, a key indicator of geomagnetic activity, with a lag of 3-4 days.
- **Polarity Rule in Pole Regions:** The "polarity rule" phenomenon, evident in Fig. 7, showcases the opposing behaviors of coronal hole areas in the sun's north and south pole regions. This observation aligns with the understanding that coronal holes near the sun's poles often exhibit contrasting magnetic field configurations.
- **Solar Activities as Precursors:** Rapid expansions in the red zone and middle area, often triggered by solar activities like solar flares or coronal mass ejections, can be precursors to subsequent geomagnetic disturbances on Earth. This relationship emphasizes the importance of monitoring solar activities to anticipate and mitigate potential geomagnetic impacts.

In essence, the BCH model, leveraging AIA 193 images from NASA's Solar Dynamics Observatory, has proven instrumental in extracting these insights. While the findings are profound, they also underscore the need for continuous monitoring and further research, especially given the dynamic nature of the sun's corona and its far-reaching implications for Earth.

6 Prediction Results

Before diving into the experimental results, it's crucial to understand the methodology underpinning our research. Our approach harnesses deep learning, specifically the Long Short-Term Memory (LSTM) model, to predict the area of the coronal hole in the Sun's middle region. The LSTM model is particularly suited for time-series data, as it can capture long-term dependencies in sequences. By feeding the model a decade's worth of data, we train it to recognize patterns and trends in the solar corona's behavior, allowing it to make informed forecasts.

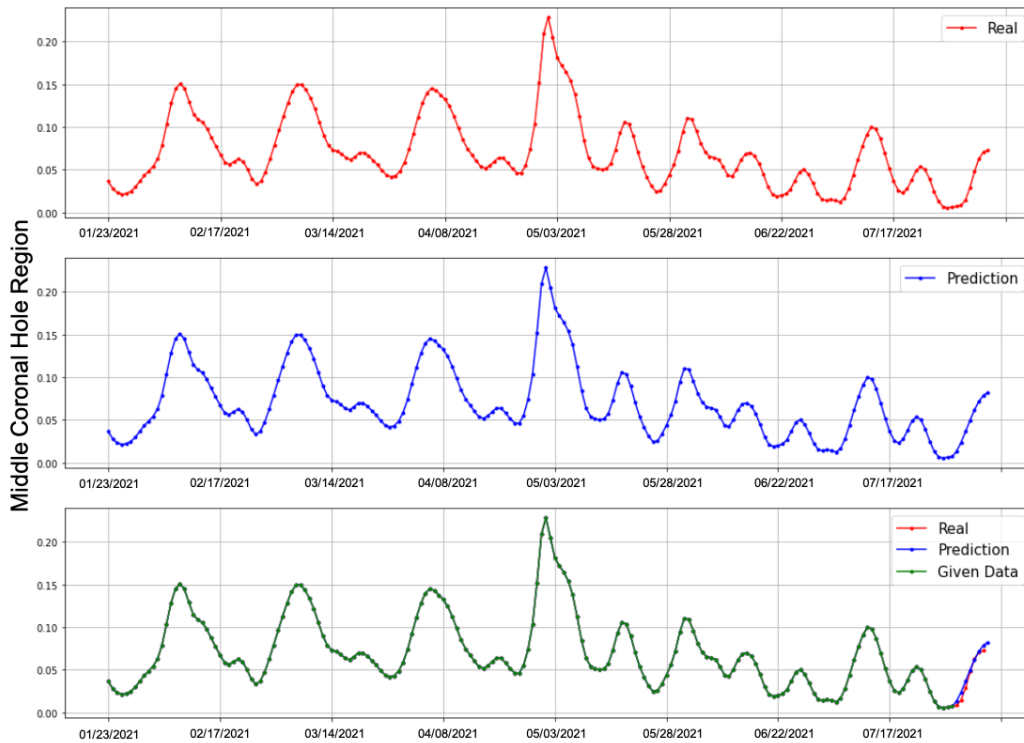


Figure 9: A comparison of actual middle area and predicted values for a 7-day period from July 31, 2021 to August 06, 2021, obtained after training the area data of 3847 middle coronal hole using LSTM from January 06, 2011 to July 30, 2021. The graph illustrates the accuracy of the LSTM model in predicting the area of the coronal hole in the middle region over a short-term period.

Now, one might wonder, why a decade? Why such an extensive dataset? The answer lies at the intersection of deep learning, solar physics, and statistical robustness. Deep learning models, especially those like LSTM, thrive on large datasets. The more data they're exposed to, the better they can generalize and predict unseen scenarios [19]. From a solar physics perspective, a decade encompasses an entire solar cycle, a period that captures the Sun's transition from solar maximum to solar minimum and vice versa. This duration ensures our model is exposed to the full gamut of solar activities, from the quietest to the most tumultuous periods [43]. Statistically, larger datasets reduce the variance of predictions, leading to more consistent and reliable outcomes [22].

Fig. 9 presents our LSTM model's attempt at predicting the area of the coronal hole in the Middle region of the Sun over a week. The predictions, while not perfect, align reasonably with the actual observations, suggesting that the LSTM can recognize and leverage patterns in the data.

Understanding and predicting the size of coronal holes is of significant interest. Their size and location can influence the emergence and trajectory of CMEs and CIRs. CMEs, essentially large bursts of solar wind and magnetic fields from the solar corona, can impact our magnetosphere when directed towards Earth. CIRs are high-speed solar wind streams that can induce geomagnetic storms and auroras [52].

By employing deep learning, particularly LSTM models, we hope to enhance space weather forecasting. The ability to anticipate the size and location of coronal holes can provide insights into potential space weather events, allowing for timely preparations.

In conclusion, our study underscores the potential of deep learning in space weather research. While our LSTM model's performance, trained on a decade of data, is promising, the sun's behavior is influenced by a myriad of factors. Thus, while a decade of data has provided insights, longer datasets might further enrich our understanding and predictions.

7 Conclusions

A streamlined model for detecting coronal holes is paramount for advancing our comprehension of space weather events and enhancing space weather forecasting accuracy. Coronal holes, distinctively marked by their low temperature and density in the sun's corona, have a notable relationship with solar winds. These winds can potentially affect Earth's satellite functions and its power grids. Hence, determining the expanse of the coronal hole is pivotal to predict space weather occurrences and to decrease their potential negative effects.

Our research has led to the formulation of a model that detects coronal holes, facilitating the accumulation of 3857 data entries related to them. This data served as the foundation for a deep learning prediction model tailored for assessing the size of the coronal holes. The incorporation of advanced deep learning tools, particularly LSTM models, for forecasting space weather series data has exhibited encouraging outcomes. This model adeptly estimates the size of the coronal hole utilizing purely numerical information.

Utilizing this model, we're better equipped to predict space weather occurrences and thereby bolster our preventive measures against their potential impacts on Earth's spatial and technological ecosystems. Additionally, forecasting the dimensions and positioning of these coronal holes enhances our grasp on the causative factors behind solar activities like CMEs and CIRs.

7.1 Study Limitations

The conclusions of this research come with a few caveats. The model is singularly focused on estimating the area of the coronal hole, sidelining other astronomical aspects that might play a part in determining its size and position. The data considered spans a decade, which may not represent the full fluctuation of the coronal hole in relation to the solar cycle. An all-encompassing comprehension necessitates data covering more extensive periods.

Our focus was primarily on mid-zones, bypassing other areas like the equatorial zone where coronal holes might manifest. Subsequent studies should shed light on these holes in varied regions and their association with space weather activities. Enriching the model's precision could be achieved by integrating data from a wider range of instruments and observatories.

7.2 Future Research

As we look forward, it's essential to delve deeper into the intrinsic physical processes dictating the genesis and evolution of coronal holes. This would require an in-depth exploration of the sun's magnetic dynamics, its influence on coronal holes, and the origins of the rapid solar wind streams they induce. There's also a pressing need for more advanced prediction tools that cover longer durations like the solar cycle, integrating expansive datasets and refined machine learning methodologies.

In addition, understanding how coronal holes impact other planets in our solar system could offer valuable perspectives on their influence on celestial entities. Persistent efforts in this domain will undoubtedly refine our predictive capabilities for space weather occurrences and augment our knowledge of the intricate space weather systems impacting Earth.

References

- [1] Abramenko, V.I., Biktimirova, R.A. Magnetic Field of Coronal Holes During the Polarity Reversal. *Geomagn. Aeron.* 62, 869–872 (2022). <https://doi.org/10.1134/S0016793222070039>.

-
- [2] Badruddin, A., and Falak, Z., (2016). Study of the geoeffectiveness of coronal mass ejections, corotating interaction regions and their associated structures observed during Solar Cycle 23. *As-trophys. Space Sci.* 361 (8), 253–316. <http://dx.doi.org/10.1007/s10509-016-2839-4>.
- [3] Baker, D. N., et al. (2002). How to cope with space weather. *Science*, 297(5586), 1486-1487.
- [4] Bartels, J., (1938). Potsdamer erdmagnetische Kennziffern, 1. Mitteilung. *Zeitschrift für Geo-physik*, 14, 68–78. <https://doi.org/10.23689/figeo-3165>.
- [5] Bartels, J., (1949). The standardized index, Ks, and the planetary index, Kp. *IATME Bull.*, 12b, 97–120.
- [6] Bengio, Y., (1994). Learning long-term dependencies with gradient descent is difficult. *IEEE Transactions on Neural Networks*, 5(2), 157-166. <http://dx.doi.org/10.1109/72.279181>.
- [7] Bobrov, M. S., (1983), Non-recurrent geomagnetic disturbances from high-speed streams, *Planet. Space Sci.*, 31, 865.
- [8] Boteler, D. H. (1998). The superstorms of August/September 1859 and their effects on the telegraph system. *Advances in Space Research*, 22(1), 13-19.
- [9] Boteler, David., (2013). Space Weather Effects on Power Systems. <http://dx.doi.org/10.1029/GM125p0347>.
- [10] Buades, A., Coll, B., and Morel, J. M., (2005). A non-local algorithm for image denoising. *In 2005 IEEE Computer Society Conference on Computer Vision and Pattern Recognition (CVPR'05)*., 2, 60-65. <http://dx.doi.org/10.1109/CVPR.2005.38>.
- [11] Cranmer, S.R., (2009). Coronal Holes. *Living Rev. Sol. Phys.* 6, 3. <https://doi.org/10.12942/lrsp-2009-3>.
- [12] Davis, K., (1990). *Ionospheric Radio*. Peter Peregrinus Ltd. London, UK.
- [13] Eoin P. Carley, Nicole Vilmer, Angelos Vourlidas., (2020). Radio Observations of Coronal Mass Ejection Initiation and Development in the Low Solar Corona. *Frontiers in Astronomy and Space Sciences*, 7, 79. <https://doi.org/10.3389/fspas.2020.551558>.
- [14] Filjar, R., (2001). Horizontal GPS Positioning Accuracy During the 1999 Solar Eclipse. *The Journal of Navigation*, 54:293–296. Cambridge University Press.
- [15] Filjar, R., T. Kos., (2006). GPS Positioning Accuracy in Croatia during the Extreme Space Weather Conditions in September 2005. *European Navigation Conference ENC 2006*. Manchester, UK.
- [16] Filjar, R., (2008). A Study Of Direct Severe Space Weather Effects On GPS Ionospheric Delay. *Journal of Navigation*, 61(1), 115-128. <http://dx.doi.org/10.1017/S0373463307004420>.
- [17] Gonzalez, R. C., & Woods, R. E. (2006). *Digital image processing* (3rd ed.). Boston, MA: Pearson Education.
- [18] Gonzalez, W. D., et al. (1994). What is a geomagnetic storm?. *Journal of Geophysical Research: Space Physics*, 99(A4), 5771-5792.
- [19] Goodfellow, I., Bengio, Y., Courville, A., & Bengio, Y. (2016). *Deep learning* (Vol. 1). MIT press Cambridge.
- [20] Gopalswamy, N., et al. (2006). Coronal mass ejections and other extreme characteristics of the 2003 October–November solar eruptions. *Journal of Geophysical Research: Space Physics*, 111(A6).
- [21] Gosling, J. T. (1996). Coronal mass ejections and magnetic flux ropes in interplanetary space. *Physics of magnetic flux ropes*, 343, 343-364.
- [22] Hastie, T., Tibshirani, R., & Friedman, J. (2009). *The elements of statistical learning: data mining, inference, and prediction*, Springer Science & Business Media.
- [23] B Heber, T.R Sanderson, M Zhang., (1999). Corotating interaction regions, *Advances in Space Research*, 23, 3, 567-579. [https://doi.org/10.1016/S0273-1177\(99\)80013-1](https://doi.org/10.1016/S0273-1177(99)80013-1).
- [24] Heinemann, M., Barra, V., Neupert, W. M., & Koza, J., (2019). Detection of coronal holes from SDO/AIA EUV images. *Astronomy and Astrophysics*, 627, A78. <http://dx.doi.org/10.1051/0004-6361/201834235>.

-
- [51] Sepp Hochreiter, Jürgen Schmidhuber., (1997). Long Short-Term Memory. *Neural Computation.*, 9 (8): 1735–1780. <https://doi.org/10.1162/neco.1997.9.8.1735>.
- [26] Inoue, S., (2016). Magnetohydrodynamics modeling of coronal magnetic field and solar eruptions based on the photospheric magnetic field. *Prog. in Earth and Planet. Sci.* 3, 19. <https://doi.org/10.1186/s40645-016-0084-7>.
- [27] Jarolim, R., Veronig, A. M., Hofmeister, S., Heinemann, S. G., Temmer, M., Podladchikova, T., & Dissauer, K. (2021). Multi-channel coronal hole detection with convolutional neural networks. *Astronomy & Astrophysics*, 652, A13. DOI: <https://doi.org/10.1051/0004-6361/202140640>
- [28] Kahler, S. W. (2001). Solar flares and coronal mass ejections. *Annual Review of Astronomy and Astrophysics*, 39(1), 351-383.
- [29] Kappenman, J. G., (1996). Geomagnetic storms and their impact on power systems. *IEEE Power Engineering Review*. 16, 5, 46-53. <https://doi.org/10.1109/MPER.1996.491910>
- [30] Lemen, J.R., Title, A.M., Akin, D.J. et al., (2012) The Atmospheric Imaging Assembly (AIA) on the Solar Dynamics Observatory (SDO). *Sol Phys* 275, 17–40. <https://doi.org/10.1007/s11207-011-9776-8>
- [31] Lipton, Z. C., Koc, K., & Bao, J. (2015). A critical review of recurrent neural networks for sequence learning. *arXiv preprint*
- [32] Linker, J. A., Heinemann, S. G., Temmer, M., Owens, M. J., Caplan, R. M., Arge, C. N., Asvestari, E., Delouille, V., Downs, C., & Hofmeister, S. J. (2021). Coronal Hole Detection and Open Magnetic Flux. *The Astrophysical Journal*, 918(1), 21. DOI: 10.3847/1538-4357/ac090a
- [33] Marr, D., (1980). Theory of edge detection. *Proceedings of the Royal Society of London B: Biological Sciences*, 207(1167), 187-217. <https://doi.org/10.1098/rspb.1980.0020>
- [34] Matzka, J., Stolle, C., Yamazaki, Y., Bronkalla, O., & Morschhauser, A., (2021). The geomagnetic Kp index and derived indices of geomagnetic activity. *Space Weather*, 19, e2020SW002641. <https://doi.org/10.1029/2020SW002641>.
- [35] McIntosh, P. S., Willock, E. C., and Thompson, R. J. (1991). Atlas of stackplots: 1966-1987. UAG-101,” in World Data Center A for Solar-Terrestrial Physics (Boulder, CO: NOAA National Geophysical Data Center).
- [36] Mursula, K., and B. Zeiger., (1996), The 13.5-day periodicity in the sun, solar wind, and geomagnetic activity: The last three solar cycles, *J. Geophys. Res.*, 101, 27,077. <https://doi.org/10.1029/96JA02470>.
- [37] Nakagawa, Y., Nozawa, S., & Shinbori, A. (2019). Relationship between the low-latitude coronal hole area, solar wind velocity, and geomagnetic activity during solar cycles 23 and 24. *Earth Planets Space*, 71, 24. <https://doi.org/10.1186/s40623-019-1005-y>.
- [38] NASA. (n.d.). Solar Dynamics Observatory (SDO). Retrieved from <https://sdo.gsfc.nasa.gov/>.
- [39] National Oceanic and Atmospheric Administration. (n.d.). Space weather. Retrieved from <https://www.noaa.gov/education/resource-collections/space-weather>.
- [40] NOAA. (2021). AP index. Retrieved from <https://www.swpc.noaa.gov/products/geospace-indices>.
- [41] Owens, M. J., & Forsyth, R. J. (2013). The heliospheric magnetic field. *Living Reviews in Solar Physics*, 10(1), 5.
- [42] Pascanu, R., Mikolov, T., & Bengio, Y. (2013). On the difficulty of training recurrent neural networks. *International Conference on Machine Learning*, 1310-1318.
- [43] Pesnell, W. D., Thompson, B. J., & Chamberlin, P. C. (2012). The Solar Dynamics Observatory (SDO). *Solar Physics*, 275(1-2), 3-15.
- [44] Rama Rao, P. V. S., Gopi Krishna, S., Vara Prasad, J., Prasad, S. N. V. S., Prasad, D. S. V. V. D., and Niranjana, K., (2009). Geomagnetic storm effects on GPS based navigation, *Ann. Geophys.*, 27, 2101–2110, <https://doi.org/10.5194/angeo-27-2101-2009>.
- [45] Richardson, I. G., E. W. Cliver, and H. V. Cane., (2000), Sources of magnetic activity over the solar cycle: Relative importance of coronal mass ejections, high-speed streams, and slow solar wind, *J. Geophys. Res.*, 105, 18, 203.

-
- [46] Richardson, I. G., E. W. Cliver, and H. V. Cane., (2001), Sources of geomagnetic storms for solar minimum and maximum conditions during 1972–2000, *Geophys. Res. Lett.*, 28, 2569.
- [47] Sandford, W. H., (1999). The Impact on Solar Winds on Navigation Aids. *The Journal. of Navigation*, 52, 42–46.
- [48] Schwenn, R., (2006) Space Weather: The Solar Perspective. *Living Rev. Sol. Phys.* 3, 2. <https://doi.org/10.12942/lrsp-2006-2>.
- [49] Y. Tian and L. Pan., (2015). Predicting Short-Term Traffic Flow by Long Short-Term Memory Recurrent Neural Network. *IEEE International Conference on Smart City*, 153-158. <https://doi.org/10.1109/SmartCity.2015.63>.
- [50] Torres, J.F., Martínez-Álvarez, F. & Troncoso., (2022). A deep LSTM network for the Spanish electricity consumption forecasting. *Neural Comput & Applic*, 34, 10533–10545. <https://doi.org/10.1007/s00521-021-06773-2>.
- [51] Sepp Hochreiter, Jürgen Schmidhuber., (1997). Long Short-Term Memory. *Neural Computation.*, 9 (8): 1735–1780. <https://doi.org/10.1162/neco.1997.9.8.1735>.
- [52] Webb, D.F., Howard, T.A., (2012). Coronal Mass Ejections: Observations. *Living Rev. Sol. Phys.* 9, 3. <https://doi.org/10.12942/lrsp-2012-3>.
- [53] Yang, B., Sun, S., Li, J., Lin, X., & Tian, Y. (2019). Traffic flow prediction using LSTM with feature enhancement. *Neurocomputing*, 332, 320-327. <https://doi.org/10.1016/j.neucom.2018.12.016>
- [54] Yashiro, S., N. Gopalswamy, G. Michalek, O. C. St. Cyr, S. P. Plunkett, N. B. Rich, and R. A. Howard (2004). A catalog of white light coronal mass ejections observed by the SOHO spacecraft, *Journal of Geophysical Research*, 109, A07105, <https://doi.org/10.1029/2003JA010282>.
- [55] Zhang, J., & Dere, K. P. (2007). A statistical study of main and residual accelerations of coronal mass ejections. *Astronomy & Astrophysics*, 464(2), 709-717.